AIP | Physics of Plasmas

E × B shear pattern formation by radial propagation of heat flux wavesa)

Y. Kosuga, P. H. Diamond, G. Dif-Pradalier, and Ö. D. Gürcan

Citation: Physics of Plasmas (1994-present) **21**, 055701 (2014); doi: 10.1063/1.4872018
View online: http://dx.doi.org/10.1063/1.4872018
View Table of Contents: http://scitation.aip.org/content/aip/journal/pop/21/5?ver=pdfcov
Published by the AIP Publishing

$E \times B$ shear pattern formation by radial propagation of heat flux waves[a)]

Y. Kosuga,[1,2,b),c)] P. H. Diamond,[1,3] G. Dif-Pradalier,[4] and Ö. D. Gürcan[5]
[1]*WCI Center for Fusion Theory, NFRI, Daejeon, South Korea*
[2]*IAS and RIAM, Kyushu University, Fukuoka, Japan*
[3]*CASS and CMTFO, University of California, San Diego, California 92093, USA*
[4]*CEA, IRFM, Paul-lez-Durance Cedex, France*
[5]*Laboratoire de Physique des Plasmas, Ecole Polytechnique, Palaiseau, France*

(Received 22 November 2013; accepted 28 December 2013; published online 23 April 2014)

A novel theory to describe the formation of $E \times B$ flow patterns by radially propagating heat flux waves is presented. A model for heat avalanche dynamics is extended to include a finite delay time between the instantaneous heat flux and the mean flux, based on an analogy between heat avalanche dynamics and traffic flow dynamics. The response time introduced here is an analogue of the drivers' response time in traffic dynamics. The microscopic foundation for the time delay is the time for mixing of the phase space density. The inclusion of the finite response time changes the model equation for avalanche dynamics from Burgers equation to a nonlinear telegraph equation. Based on the telegraph equation, the formation of heat flux jams is predicted. The growth rate and typical interval of jams are calculated. The connection of the jam interval to the typical step size of the $E \times B$ staircase is discussed. © *2014 AIP Publishing LLC*. [http://dx.doi.org/10.1063/1.4872018]

I. INTRODUCTION

Formation of $E \times B$ flow patterns is often observed in magnetized plasmas.[1–3] Examples include, but are not limited to, the formation of edge shear flows by transport bifurcation,[4,5] the formation of zonal flows in drift wave turbulence,[2,3] etc. Recently, a new class of $E \times B$ flow patterns, the $E \times B$ staircase (Fig. 1), was observed in gyrokinetic simulations of flux driven, full f ion temperature gradient (ITG) turbulence using GYSELA.[6] An $E \times B$ staircase is a quasi-regular pattern of profile corrugations and shear flows. In the regions between corrugations, transport is non-local,[7–16] $Q = -\int dx' \chi(x, x') \nabla T(x')$, with the kernel width $\Delta \gg \Delta_c$ corresponding to the distance between steps. Here, Δ_c is the turbulence correlation length. Transport in these regions is dominated by stochastic avalanches,[9,17–19] which are distributed with outer scale Δ. The entire pattern of the corrugations and the steps co-existing with avalanches was named the $E \times B$ staircase, after potential vorticity (PV) staircases in geophysical fluid dynamics.[20,21]

The emergence of $E \times B$ staircases in gyrokinetic simulations is not so surprising, since it is a natural consequence of phase space density mixing, which is analogous to potential vorticity mixing in geophysical fluid dynamics.[20–27] What is surprising here is the fact that seemingly exclusive phenomena, namely, strong $E \times B$ shear flows and stochastic avalanches, co-exist. To see this, note that on one hand, strong shear flows should reduce avalanche transport. On the other, avalanches can be strong enough to smooth out corrugations by transporting heat, and thus may break the $E \times B$ "barrier." Surprisingly, these two mutually exclusive phenomena can survive side-by-side in $E \times B$ staircases. The co-existence is achieved by self-organizing the entire profile into the two distinct regions, one where avalanches of the size $\Delta \gg \Delta_c$ dominate, and the other where corrugations and shear flows are localized. However, the emergence of $E \times B$ staircases cannot be described using the usual quasi-linear modulation theory for $E \times B$ flow generations in magnetized plasmas. For example, the "eigenfunction" idea[3] seems inappropriate here, since staircases do not grow simultaneously throughout the entire region. Rather, staircases start forming at one location and then continue self-assembling step-by-step. A more specific issue here is to explain the emergence of particular scales, such as the staircase step size. Here, we cannot directly relate the typical scale to the Rhines scale,[28] since that scale has nothing to do with stochastic avalanches, and is based on inverse cascade inertial range physics. We also note that other theories[18,19,29] do not account for the emergence of a particular scale apart from those already present in the models.

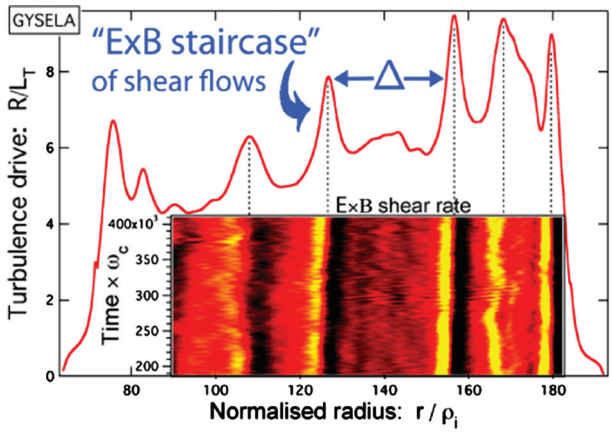

FIG. 1. An $E \times B$ staircase. Here, temperature gradient is plotted against the plasma radius. At steady state of the simulation, the temperature profile is corrugated. The strong corrugations were accompanied by strong $E \times B$ shears, as shown in the lower part of the figure. In the regions between the corrugations, or "steps," transport were found to be non-local and dominated by avalanches.[6]

[a)]Paper JI2 1, Bull. Am. Phys. Soc. **58**, 143 (2013).
[b)]Invited speaker.
[c)]Electronic mail: kosuga@riam.kyushu-u.ac.jp

TABLE I. Comparison of heat avalanche dynamics and traffic jam dynamics. In plasmas, the instantaneous heat flux can deviate from the mean flux around the marginal state. The heat flux adjusts its value toward the mean value in a finite response time τ. The response time is an analogue of drivers' response time in traffic, during which each driver adjusts speed to that of a mean background traffic flow.[31]

	Heat avalanche	Traffic flow
Dynamical variable (order parameter)	Deviation from marginal profile δT	Car density perturbation $\delta\rho$
Instantaneous flux	Heat flux Q	Traffic flow v
Mean Flux	$Q_0[\delta T] \rightarrow$ Mean flux near marginality determined by symmetry constraints or $\rightarrow$ quasilinear flux	$V(\delta\rho) - (\nu/\rho)\partial_x\delta\rho$ background traffic flow, determined empirically or by general consideration
Response time	Mixing time during which instantaneous heat flux relaxes to the mean flux	Drivers' response time during which drivers adjust their speed to the surrounding traffic speed

In this paper, we propose a model to describe the generation of $E \times B$ staircases by extending the theory for avalanche dynamics. In developing the theory, we consider that heat flux waves can "jam" to corrugate profiles and produce shear layers. To reveal such an effect, a key is to consider the finite time delay[30,31] between the instantaneous heat flux and the mean flux. As shown in Table I, the response time is an analogue of the drivers' reaction time in traffic flows.[32,33] By including finite response time, the model for heat avalanche dynamics is extended from Burgers equation to the nonlinear telegraph equation (Fig. 2). As the telegraph equation has both a second time derivative due to the finite response and a second spatial derivative due to ambient diffusion, it naturally introduces *waves* into the dynamics of meso-scale heat perturbations. The heat flux waves propagate at a typical speed $\sqrt{\chi_2/\tau}$, where χ_2 is ambient thermal diffusion and τ is the response time. The waves are immersed in the bath of propagating pulses at speed $c_0 \sim \lambda\delta T$ (Fig. 3). When the response time is short, and thus when heat flux waves propagate faster than a pulse, the pulse is left behind. The dynamics of the pulse is described by Burgers equation. However, when the response time is long, pulses can *overtake* the heat flux waves. In this case, a heat flux jam can happen, just as a traffic jam can happen for a long drivers' reaction time.[32,33] A heat flux jam may be thought of as clustering instability,[32,33] where the effective conductivity $\chi_2 - c_0^2\tau$ can be negative in the case of overtaking ($c_0 > \sqrt{\chi_2/\tau}$). The growth rate is calculated, which allows prediction of a particular scale favored by the jam instability. The scale for the maximal growth is obtained and is typically $\Delta^2 \sim \rho_i\sqrt{\chi_2\tau}$. Here, Δ is determined by the geometric mean of ρ_i and $\sqrt{\chi_2\tau}$, the propagation length of the heat flux wave in 1 response time. We quantitatively evaluate the scale for a saturated state achieved via shearing feedback from the resulting staircase. The result indicates that the typical scale is $\Delta \sim 10\Delta_c$, which is comparable to the spacing between corrugations in staircases (Fig. 1).

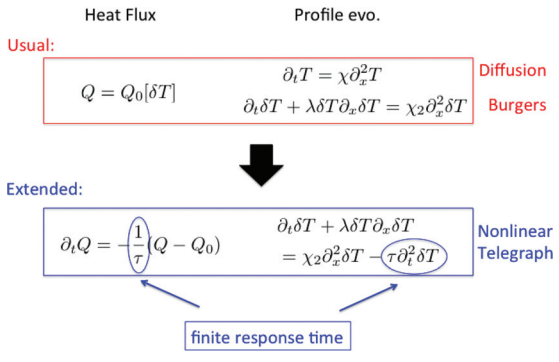

FIG. 2. Extension of heat evolution equation from diffusion/Burgers equation to the nonlinear telegraph equation. Here, the extension is made by introducing the finite response time τ, during which plasmas adjust the heat flux toward the mean value. Physically, the response time is an analogue of drivers' response time. Formally, it is a natural consequence of phase space density mixing. Note that the latter lays the microscopic foundation for introducing the response time.

The remainder of the paper is organized as follows. In Sec. II, we discuss an extension of the model for heat avalanche dynamics to include the finite response time. The physical idea and microscopic foundation for the response time are presented. In Sec. III, we present an analysis based on the extended model. Heat perturbation dynamics is analyzed using the telegraph equation. Section IV contains the conclusion and discussion.

II. MODEL

Here, we derive a model to describe *avalanche dynamics* with a time delay between heat flux and temperature perturbations. We first present a brief summary of the conventional avalanche dynamics theory based on the idea of joint reflection symmetry.[18,19] We then discuss the extension of the heat avalanche dynamics model to include finite delay time. The physical idea behind the finite time delay is explained, based on the analogy of the model to traffic jam evolution. We also discuss the microscopic origin of the time delay, by considering the mixing of phase space density.

In previous studies,[18,19] theory of avalanche dynamics was developed based on symmetry arguments. In this line of

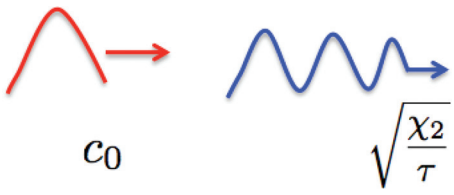

FIG. 3. A schematic drawing for a pulse propagating at c_0 and a heat flux wave train propagating at $\sqrt{\chi_2/\tau}$. Depending on pulse amplitude ($c_0 \propto \delta T$) and the response time, one of these two can propagate faster than the other. For short response time limit, heat flux waves propagate faster. For long response time, the heat flux wave speed becomes slower and finally pulses can overtake the wave front.

approach, the deviation from the marginal profile serves as a conserved order parameter. For example, the evolution of the temperature deviation is given by

$$\partial_t \delta T + \partial_x Q[\delta T] = 0. \tag{1}$$

Here, $Q[\delta T]$ is the turbulent heat flux. The total heat flux is determined by the sum of the turbulent flux and the neoclassical flux, $Q_{tot} = Q + Q_{neo}$. Here, we consider a regime where the transport is due to turbulence, so Q_{neo} is negligible. Thus, this model does not apply to transport within an already existing ITB. To close the equation, we need a specific form of $Q[\delta T]$. To determine its form, we require that the net transport must be down the gradient (Fig. 4). This requires that blobs (local excess) must propagate outward, while holes (local deficit) must propagate inward. In order to allow these types of solutions, the basic equation must be invariant under the transformations $x \to -x$ and $\delta T \to -\delta T$. The general form that satisfies joint reflection symmetry is

$$Q[\delta T] = \sum_{p,q,r} \{A_{2p} (\delta T)^{2p} + B_{q,r} \partial_x^q \delta T^r + ...\}, \tag{2}$$

where p, q, and r are integers and $q + r$ must be even. The simplest, non-trivial flux is

$$Q_0[\delta T] = \frac{\lambda}{2} (\delta T)^2 - \chi_2 \partial_x \delta T + \chi_4 \partial_x^3 \delta T. \tag{3}$$

To the lowest non-trivial order, the dynamics of the temperature deviation is given as

$$\partial_t \delta T + \lambda \delta T \partial_x \delta T = \chi_2 \partial_x^2 \delta T. \tag{4}$$

This is a Burgers equation for the deviation from the marginal profile. The dynamics of heat avalanches was analyzed based on Eq. (4).[18,19] It was argued that large avalanches of system size a dominate transport.

Here, as an extension of the heat avalanche model, we admit the possibility of a finite time deviation of the instantaneous heat flux Q from the mean heat flux Q_0, where the latter is determined by the symmetry constraint. As demonstrated by simulations,[6,34] the heat flux has intrinsic variability around a mean value. Thus, the instantaneous heat flux can differ from the mean heat flux. This difference relaxes due to phase space density mixing. The dynamics of such heat flux evolution can be modeled as

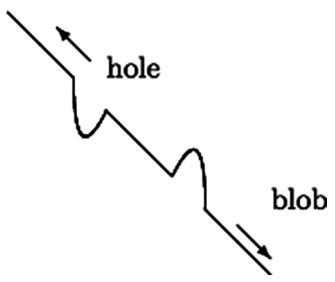

FIG. 4. Schematics for blobs propagating outward and holes propagating inward. These are allowed to have net transport down the gradient. To have both solutions, equation must be invariant under the simultaneous transformation of $x \to -x$ and $\delta T \to -\delta T$.

$$\partial_t Q = -\frac{1}{\tau} (Q - Q_0[\delta T]). \tag{5}$$

Here, τ is the plasma response time during which the instantaneous heat flux relaxes toward the specified mean value. The physical idea behind the model extension may be clarified by invoking the similarity of heat avalanche dynamics to traffic flow dynamics (Table I). A well known simple model[32,33,35] for 1D traffic flow dynamics is given by

$$\partial_t \rho + \partial_x (\rho v) = 0, \tag{6}$$

$$\partial_t v + v \partial_x v = -\frac{1}{\tau} \left(v - V(\rho) + \frac{\nu}{\rho} \partial_x \rho \right). \tag{7}$$

Here, ρ is the local car density, v is the speed of each car, $V(\rho)$ is the mean background traffic flow, ν is the diffusivity, and τ is the drivers response time. The similarity between traffic flow dynamics and heat avalanche dynamics is clear. In traffic flow, the instantaneous speed of individual cars can deviate from the mean background traffic flow. When the two speeds are different, drivers respond to the difference by adjusting their speed toward the mean value in a time τ. Similarly, in plasmas, the instantaneous heat flux Q can deviate from the mean heat flux. We show that plasmas adjust the heat flux toward the mean value in the plasma response time τ. The plasma response time τ is the analogue of the drivers' response time. As we will show later, the plasma response time originates from phase space density mixing. When the response time is long, traffic jams can form.[32] The process of traffic jam formation results from a clustering instability, which occurs when $\tau > \nu / c_0^2$, where c_0 is the initial streaming speed. Later, we show that the heat flux can also jam in the limit of long plasma response time.

While the heuristic argument given above clarifies the physical picture of the response time, its microscopic origin and quantitative features also must be established. In order to answer this question, here we present a more formal derivation of the response time from microscopic physics. To proceed, we note that plasma turbulence conserves phase space density, $df/dt = 0$, up to collisions. A relaxation process mixes phase space density and enhances turbulent fluctuations. That process leads to the production of fluctuation "phasetrophy,"[36] as measured by the 2 point phase space density correlation $\langle \delta f(1) \delta f(2) \rangle_+$. Here, the average is over the center of mass coordinate $\mathbf{x}_+ = (\mathbf{x}_1 + \mathbf{x}_2)/2$. To be more specific, here we consider a simplified model for gyrokinetic turbulence[37]

$$\partial_t f + v_D \bar{E} \partial_y f + \tilde{\mathbf{v}}_{E \times B} \cdot \nabla f = 0, \tag{8}$$

where $v_D \bar{E}$ is the energy dependent drift. For this model, the phasetrophy evolution is given as

$$\partial_t \langle \delta f(1) \delta f(2) \rangle_+ + \frac{1}{\tau_{mix}} \langle \delta f(1) \delta f(2) \rangle_+ = P(1,2) \tag{9}$$

and

$$P(1,2) = -\langle \tilde{v}_x(1) \delta f(2) \rangle_+ \langle f \rangle'(1) - \langle \tilde{v}_x(2) \delta f(1) \rangle_+ \langle f \rangle'(2). \tag{10}$$

Here, $P(1,2)$ describes the *production* of fluctuation phasetrophy by the relaxation of free energy in the system. τ_{mix} is the mixing time of phasetrophy, which is determined by synergy of the drift and $E \times B$ mixing[38]

$$\frac{1}{\tau_{mix}}\langle \delta f(1)\delta f(2)\rangle_+ = v_{Di}E_1\frac{\partial}{\partial y_1}\langle \delta f(1)\delta f(2)\rangle_+ + \nabla_1 \cdot \langle \tilde{\mathbf{v}}(1)\delta f(1)\delta f(2)\rangle_+ + (1 \leftrightarrow 2). \tag{11}$$

Here, $(1 \leftrightarrow 2)$ denotes the terms with the arguments exchanged. τ_{mix} is typically on the order of the turbulent phase space density correlation time.[38] Associated with phasetrophy mixing, the heat flux is also relaxing toward a specified value. This can be seen by differentiating Eq. (9) with respect to y_2, multiplying E_1, and then taking the velocity moment to obtain

$$\partial_t \int d^3v_1 d^3v_2 E_1 \langle \delta f(1)\partial_{y_2}\delta f(2)\rangle_+ + \frac{1}{\tau_{mix}}\int d^3v_1 d^3v_2 E_1 \langle \delta f(1)\partial_{y_2}\delta f(2)\rangle_+ = \int d^3v_1 d^3v_2 E_1 \partial_{y_2} P(1,2). \tag{12}$$

Noting $\int d^3v \partial_y \delta f = \partial_y \delta n \propto \tilde{v}_x$ for adiabatic electrons ($\delta n \sim \tilde{\phi}$) and considering flat density (i.e., $\int dv_2^3 \langle f\rangle'(2) \to 0$) for simplicity, we have

$$\partial_t Q = -\frac{1}{\tau_{mix}}(Q - Q_0), \tag{13}$$

where $Q = \langle \tilde{v}_x \delta T\rangle_+$ is the turbulent heat flux and $Q_0 = -\tau_{mix}\langle \tilde{v}_x^2\rangle \langle T\rangle'$ is the mean heat flux, here described by Fick's law. Thus, the heat flux evolves in time during the phase space density mixing process. It is important to note that the above consideration reveals that the typical scale of the response time is on the order of the turbulent mixing rate. Also, the microscopic origin of the response time is now clear. The deviation of instantaneous heat flux from the specified mean flux is a natural consequence of phase space density mixing.

Given the physical picture and microscopic foundation, an extended model for heat avalanche dynamics emerges as

$$\partial_t \delta T + \partial_x Q = 0, \tag{14}$$

$$\partial_t Q = -\frac{1}{\tau}(Q - Q_0[\delta T]), \tag{15}$$

where $Q_0[\delta T]$ is the mean flux determined by joint reflection symmetry (Eq. (3)). Eliminating the heat flux, we obtain the evolution equation for the temperature perturbation as

$$\partial_t \delta T + \lambda \delta T \partial_x \delta T = \chi_2 \partial_x^2 \delta T - \chi_4 \partial_x^4 - \tau \partial_t^2 \delta T. \tag{16}$$

Equation (16) describes the dynamics of the temperature deviation from the marginal profile, including a finite response time. Comparing to previous models for avalanche dynamics, here the equation has developed from a Burgers equation to a nonlinear telegraph equation (See Fig. 2). We note that the telegraph equation has been also derived for drift wave-zonal flow turbulence.[39] In that study, a telegraph equation was derived for zonal flow shear evolution by including finite response time in the momentum flux evolution. The telegraph equation was used to describe a novel oscillatory behavior of drift wave-zonal flow turbulence.

III. ANALYSIS

Here, we present the analysis of the telegraph equation. At the outset, it is important to note that there are two characteristic speeds in the telegraph equation (Fig. 3). Since there are two characteristic speeds in the problem, the behavior of solutions can differ, depending which speed is faster. Here, we discuss the characteristic behavior of heat perturbations in both limits.

We start with the familiar limit with short response time, where heat flux waves propagate faster than heat pulses. Since telegraph equations reduce to Burgers equations in this limit, we expect that front-like solutions can be found. Indeed, we can find propagating exact solutions as follows. To find propagating solutions, we substitute $\delta T(x - ct)$ into the telegraph equation, to obtain

$$-c\delta T' + \lambda \delta T \delta T' = (\chi_2 - c^2\tau)\delta T''. \tag{17}$$

Here, the prime denotes derivative with respect to $\xi \equiv x - ct$. Note that the same relation is obtained from Burgers equation with viscosity replaced by $\chi_2 - c^2\tau$. Indeed, in the short response time limit, the mathematical structure is identical to that of Burgers. Equation (17) can be integrated using the methods for Burgers equation. For the boundary conditions such that $\delta T' \to 0$, $\delta T \to \delta T_\pm$ as $\xi \to \pm\infty$, and $\delta T_- > \delta T_+$, Eq. (17) can be integrated to give

$$\delta T = \frac{\delta T_- + \delta T_+ \exp\left(\frac{\lambda}{2}\frac{\delta T_- - \delta T_+}{\chi_2 - c\tau^2}\xi\right)}{1 + \exp\left(\frac{\lambda}{2}\frac{\delta T_- - \delta T_+}{\chi_2 - c\tau^2}\xi\right)}. \tag{18}$$

Here, $c = (\lambda/2)(\delta T_- + \delta T_+)$. Equation (18) describes ballistically propagating front solutions. Typical propagating patterns are shown in Fig. 5. If $\delta T_- > 0$ and $\delta T_+ \to 0$, $c = \lambda \delta T_-/2 > 0$ and Eq. (18) describes a hot front propagating outward. This is a blob-like solution.[10,11] On the other hand, if $\delta T_- \to 0$ and $\delta T_+ = -|\delta T_+| < 0$, we have $c = -\lambda|\delta T_+|/2 < 0$ and thus Eq. (18) describes a cold front

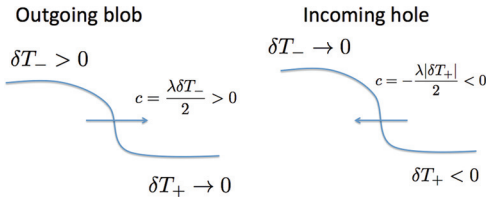

FIG. 5. A schematic drawing for front solutions. For $\delta T_- > 0$ and $\delta T_+ \to 0$, we have heat excess propagating outward at $c = \lambda \delta T_-/2 > 0$. For $\delta T_- \to 0$ and $\delta T_+ < 0$, we have heat deficit propagating inward at $c = -\lambda|\delta T_+|/2 < 0$.

(void) propagating inward. In both cases, the propagation speeds are proportional to amplitude. Thus, hotter blobs or colder holes propagate faster. This is analogous to the behavior of front-like solutions in Burgers turbulence.

On the other hand, in the limit of the long response time, pulses can overtake heat flux waves (Fig. 3). As we see below, heat flux jams can happen in this situation. This is physically plausible, since this limit is analogous to flows of traffic where the drivers have a long response time. In order to analyze such effects, we consider an avalanche initially propagating at the speed $c_0 = \lambda\delta T_0$ and examine whether a perturbation on it grows or not. The perturbation evolves in time as

$$\partial_t\widetilde{\delta T} + c_0\partial_x\widetilde{\delta T} = \chi_2\partial_x^2\widetilde{\delta T} - \chi_4\partial_x^4\widetilde{\delta T} - \tau\partial_t^2\widetilde{\delta T}. \tag{19}$$

In the frame of the pulse, the righthand side reads as $(\chi_2 - c_0^2\tau)\partial_x^2\widetilde{\delta T} - \chi_4\partial_x^4\widetilde{\delta T}$. Thus in the long response time limit, the effective conductivity can be negative and we expect an instability to develop. This is analogous to a clustering instability of cars in traffic, i.e., a "pile-up." Here, *heat* perturbations can cluster to form a "*heat flux jam.*" Note also that the negative conductivity instability is analogous to the familiar negative viscosity for zonal flow formation.[3] In the case of zonal flow formation, zonal flows arise as secondary modes formed by an ensemble of primary drift waves. In the case of jam formation, heat flux jams, or *"jamitons,"*[33] evolve as a secondary mode driven by the primary ensemble of avalanches.

The growth rate of heat jam formation is obtained by Fourier analyzing Eq. (19)

$$\omega_{r,k} = \pm\frac{1}{2\tau}\sqrt{\frac{r-1}{2} + 2\tau\chi_2k^2\left(1+\frac{\chi_4k^2}{\chi_2}\right)}, \tag{20}$$

$$\gamma_k = -\frac{1}{2\tau} + \frac{1}{2\tau}\sqrt{\frac{r+1}{2} - 2\tau\chi_2k^2\left(1+\frac{\chi_4k^2}{\chi_2}\right)}, \tag{21}$$

where $r \equiv \sqrt{\left\{4\tau\chi_2k^2(1+\chi_4k^2/\chi_2) - 1\right\}^2 + 16c_0^2k^2\tau^2}$. From this, we can see that the critical, minimal time delay required for jam growth is

$$\tau > \frac{\chi_2}{c_0^2}\left(1+\frac{\chi_4k^2}{\chi_2}\right). \tag{22}$$

Importantly, the growth rate introduces a scale dependence of heat flux jams -, i.e., we see that there is a particular scale which is optimal for heat jam formation. Note that this identifies an *emergent* scale in the problem, which is not one of the basic scales of the model. The scale for maximum growth rate can be obtained by solving $\partial\gamma_k/\partial k^2 = 0$, which gives

$$8\tau\frac{\chi_4^2}{\chi_2}k^6 + 4\tau\chi_4k^4 + 2\frac{\chi_4}{\chi_2}k^2 + 1 - \frac{c_0^2\tau}{\chi_2} = 0. \tag{23}$$

Assuming $k^2 < \chi_2/\chi_4$ to avoid stabilizing χ_4 effects gives

$$k_{max}^2 \cong \frac{\chi_2}{\chi_4}\sqrt{\frac{\chi_4c_0^2}{4\chi_2^3}} = \frac{\lambda\delta T_0}{2\sqrt{\chi_2\chi_4}}. \tag{24}$$

From this, we can calculate the scale for the maximal growth and jamming instability wavelength, which set the inter-jam spacing (Fig. 6)

$$\Delta_{max}^2 = k_{max}^{-2} = \frac{2\sqrt{\chi_2\chi_4}}{\lambda\delta T_0}, \tag{25}$$

$$\gamma_{max} \cong \frac{1}{2\tau}\sqrt{\frac{c_0^2\tau}{\chi_2}} = \frac{\lambda\delta T_0}{2\sqrt{\chi_2\tau}}. \tag{26}$$

Here, we note that the spacing can be a function of amplitude. Thus, the larger the corrugation amplitudes are, the narrower the spacing is. This property is analogous to that of typical solitons, such as for ion acoustic waves.[40] We also note that there are two characteristic scales in the nonlinear pattern shown in Fig. 6, i.e., one for the inter-jam spacing and the other for the scale of corrugations. Here, we calculate the inter-jam spacing Δ. In most cases, this scale is of greater interest since it sets the size of the largest avalanches.

In order to estimate the typical value for the scale, we assume that heat flux jam instability feedbacks on itself, by producing strong corrugations and $E\times B$ shear flows (Fig. 7). The idea behind this assumption is that strong corrugation in the profile resembles "the transport barrier" in fusion plasmas. In these cases, the steep gradient in the profile can give rise to a strong $v'_{E\times B}$, which is often associated with the suppression of instability. As a crude estimate, this feedback may be expected when the $E\times B$ shear becomes comparable to the maximal growth rate,[41] i.e., $\gamma_{max} \sim v'_{E\times B}$. Here, $v'_{E\times B}$ is supported via corrugated profiles as

$$v'_{E\times B} \cong \frac{c}{eB}\delta T'' \cong \frac{c\delta T}{eB\Delta_{max}^2} \sim \frac{\omega_{ci}\rho_i^2\lambda T_i}{2\sqrt{\chi_2\chi_4}}\left(\frac{\delta T}{T_i}\right)^2. \tag{27}$$

In this case, the scale for the maximum can be evaluated as

$$\Delta_{max}^2 \sim \frac{2v_{thi}}{\lambda T_i}\sqrt{\chi_2\tau}\rho_i. \tag{28}$$

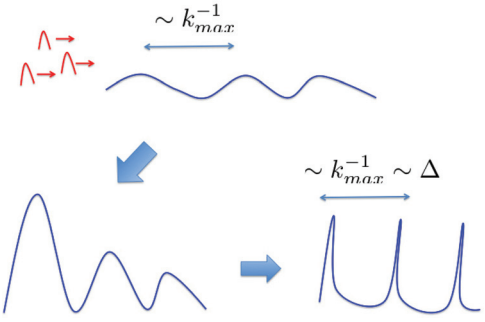

FIG. 6. A schematic view of jam growth. Heat flux waves (indicated in blue), immersed in stochastic avalanches (indicated in red), grow due to overtaking and form jams. Once the first shear layer is produced by jamming, the second layer starts to develop. The process continues. Finally, the system self-assembles into a nonlinear pattern, with sharp corrugations interspersed by Δ. Δ is closely related to the spacing in staircases.

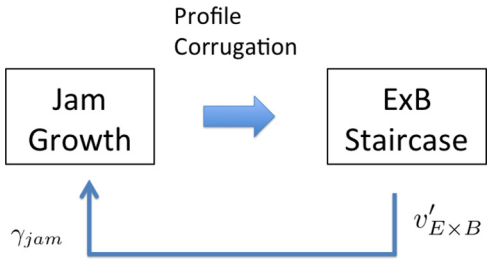

FIG. 7. A feedback loop for the jam instability leading to $E \times B$ staircases. Once jamming instability is initiated, the profile starts corrugating to produce $E \times B$ staircases. The resultant $E \times B$ shear can feedback to the original jam instability.

Note that the emergence of a scale *not* initially embedded in the theory! The typical scale is given by the *geometric mean* of the correlation length ($\sim\rho_i$) and the propagation length for heat flux waves in 1 response time $(\sqrt{\chi_2/\tau})\tau = \sqrt{\chi_2\tau}$. Using typical values, $T_i \sim 1\,\mathrm{keV}$, $n \sim 10^{13}\,\mathrm{cm}^{-3}$, $B \sim 10^4$ Gauss, $\epsilon_0 \sim 1/3$, and assuming $\lambda T_i \sim$ a pulse propagation speed $\sim 100\,\mathrm{cm}/0.1\,\mathrm{s} \sim 10^3\,\mathrm{cm/s}$, $\tau \sim \Delta\omega^{-1} \sim 10^{-5}\,\mathrm{s}$, $\chi_2 \sim \chi_{neo} \sim \nu_{ii}\rho_i^2/\epsilon_0^{3/2} \sim 1.4 \times 10^2\,\mathrm{cm}^2/\mathrm{s}$, and $\Delta_c \sim 1.5\,\mathrm{cm}$ for $k_\perp\rho_i \sim 0.2$, we have $\Delta_{max} \sim 12 \times \Delta_c \sim 18\,\mathrm{cm}$. Thus, Δ_{max} is the typical of the meso-scale range, i.e., $\Delta_c \ll \Delta < a$. Δ_{max} is also comparable to the size of staircase steps in simulations.[6,42]

IV. CONCLUSION AND DISCUSSION

In this paper, we presented an extension of the heat avalanche model and its application to the formation of the $E \times B$ staircase. The principal results of the paper are as follows.

1. We discussed an extension of the model of heat avalanches to account for the finite time delay between the instantaneous flux and the mean flux

$$Q_0[\delta T] = \frac{\lambda}{2}\delta T^2 - \chi_2\partial_x\delta T - \chi_4\partial_x^3\delta T,$$

$$\Rightarrow \partial_t Q = -\frac{1}{\tau}(Q - Q_0[\delta T]). \tag{29}$$

   Here, τ is the response time for plasmas to relax the instantaneous heat flux to the mean flux. The response time is an analogue of drivers' response time in traffic flow. The microscopic foundation for the response time was developed by considering the mixing of phase space density. The microscopic consideration also reveals that the response time is of the order of the $E \times B$ mixing time or the turbulence correlation time.
2. As a consequence of the finite response time, heat evolution is described by a *nonlinear telegraph equation*

$$\tau\partial_t^2\delta T + \partial_t\delta T + \lambda\delta T\partial_x\delta T = \chi_2\partial_x^2\delta T - \chi_4\partial_x^4\delta T. \tag{30}$$

   Here, the response time enters the second time derivative term. This, together with the diffusion term, introduces wave dynamics into the heat equation with wave speed $c = \sqrt{\chi_2/\tau}$.
3. When the response time is long, heat pulses can overtake heat flux waves. Alternatively, just as traffic jams can form when the drivers' response time is long, here a heat flux jam can form when the plasma response time is long. The typical scale associated with maximal growth was calculated (Eq. (26)). The typical value of the scale was estimated for a saturated state, which is achieved when the feedback from the $E \times B$ flow shear (from a corrugated profile) becomes comparable to the original jam growth rate. The result is $\Delta_{max}^2 \sim (2v_{thi}/\lambda T_i)\sqrt{\chi_2\tau}\rho_i$. The scale is set by the geometric mean of the Larmor radius and the heat wave propagation length in 1 response time. The result is consistent with the typical step spacing of staircases, as observed in simulations.[6,42]

Having summarized the theoretical ideas, we now discuss the connection to both *numerical* and *physical* experiments. To digitally test the theory presented here, it may be useful to study how the staircase structures respond to varying *the source intensity*. Assuming the source intensity and the temperature variability are correlated, we expect that the staircase spacing would shrink as the power input increases (Eq. (26)). Another interesting test is to examine how the staircase responds to varying *the ambient diffusion* $\chi_2 \sim \chi_{neo}$. By increasing the ambient diffusion, we expect heat flux waves to propagate faster and so overtaking to become more difficult. Thus, from the view point of jam formation, the staircase structure may not develop for large enough χ_2. Finally, we note that probing the locations of profile corrugations is an interesting test as well. As the theory does not include the effect of sheared magnetic fields, the location of corrugations in the model is not tied to the low q (the safety factor) rational surfaces. The similar tendency is obtained at least in the former simulation study.[6] More tests on the location may be useful as a basic characterization of staircases.

For physical experiments, an ideal venue in which to probe avalanche jams is plasma near the marginal state.[9] In plasmas near marginality, one might excite heat flux waves and add noise. One way to identify such heat flux waves would be to characterize the pulse propagation speed and compare it to $\sqrt{\chi_2/\tau}$. If heat flux waves exist in plasmas, then we can induce modulations and can examine whether heat flux jams form or not. These may be a possible step for identifying heat flux jamming effects in experiments.

In the future, both application of theory to different problems and further extension of the basic theory merit attention. One relevant application of the theory may be to the problem of pulse propagation studies in fusion plasmas.[7–16] Recalling that the telegraph equation naturally introduces a propagation speed $c = \sqrt{\chi_2/\tau}$ and that it suggests the existence of propagating solutions of the form $f(x - ct)$, we expect that the telegraph equation may be useful for analyzing pulse propagation phenomena. Indeed, the characteristic speed $\sqrt{\chi_2/\tau}$ is similar to that of the front in a Fisher reaction-diffusion system.[29,43–46] This is $\sqrt{\gamma D}$, where γ is growth rate and D is ambient diffusivity. Note that the latter is often invoked in the study of pulse propagation phenomena. The telegraph equation may also be applied to characterize typical propagation speeds. Further extension of the basic theory is important as well. One relevant extension is to treat the response time self-consistently. While we treated

τ as a parameter on the order of $E \times B$ mixing time, it is, in fact, a function of the turbulence amplitude, so $\tau(\mathcal{E})$. Thus, some understanding of the dynamics of the turbulence intensity is required. The extension to the self-consistent response time may be important to fully represent the effect of the "deviation" of the system from marginality. There are several other extensions, such as nonlinear analysis of the jam evolution beyond the linear regime, consideration of noise effects in the telegraph equation, and calculating the critical exponents[18,19] for jamming front propagation. In particular, the nonlinear analysis of the jam evolution, including the coupling to the dynamics of ambient turbulence *and* zonal flows, may merit more attention. Such analysis would allow more detailed feedback analysis on jam instability beyond the simple $E \times B$ shear feedback as invoked above calculation. These will be pursued in the future.

ACKNOWLEDGMENTS

We thank Z. Guo, M. E. McIntyre, X. Garbet, S.-I. Itoh, K. Itoh, S. Inagaki, M. Lesur, and the participants in the 2009, 2011, 2013 Festival de Theorie for stimulating discussions. This work was supported by the WCI project 2009-001 of MEST of Korea, Grant-in-Aid for Scientific Research of JSPF of Japan (Nos. 21224014 and 25887041), U.S. Department of Energy Grant No. DE-FG02-04ER54738.

[1]S. Champeaux and P. H. Diamond, Phys. Lett. A **288**, 214 (2001).
[2]A. Fujisawa, K. Itoh, H. Iguchi, K. Matsuoka, S. Okamura, A. Shimizu, T. Minami, Y. Yoshimura, K. Nagaoka, C. Takahashi, M. Kojima, H. Nakano, S. Oshima, S. Nishimura, M. Isobe, C. Suzuki, T. Akiyama, K. Ida, K. Toi, S. I. Itoh, and P. H. Diamond, Phys. Rev. Lett. **93**, 165002 (2004).
[3]P. H. Diamond, S.-I. Itoh, K. Itoh, and T. Hahm, Plasma Phys. Controlled Fusion **47**, R35 (2005).
[4]R. J. Groebner, K. H. Burrell, and R. P. Seraydarian, Phys. Rev. Lett. **64**, 3015 (1990).
[5]K. Ida, S. Hidekuma, Y. Miura, T. Fujita, M. Mori, K. Hoshino, N. Suguki, T. Yamaguchi, and J.-M. Group, Phys. Rev. Lett. **65**, 1364 (1990).
[6]G. Dif-Pradalier, P. H. Diamond, V. Grandgirard, Y. Sarazin, J. Abiteboul, X. Garbet, P. Ghendrih, A. Strugarek, S. Ku, and C. S. Chang, Phys. Rev. E **82**, 025401(R) (2010).
[7]K. W. Gentle, R. V. Bravenec, G. Cima, H. Gasquet, G. A. Hallock, P. E. Phillips, D. W. Ross, W. L. Rowan, A. J. Wootton, T. P. Crowley, J. Heard, A. Ouroua, P. M. Schoch, and C. Watts, Phys. Plasmas **2**, 2292 (1995).
[8]P. Mantica, P. Galli, G. Gorini, G. M. D. Hogeweij, J. de Kloe, N. J. L. Cardoza, and R. Team, Phys. Rev. Lett. **82**, 5048 (1999).
[9]P. A. Politzer, Phys. Rev. Lett. **84**, 1192 (2000).
[10]J. A. Boedo, D. Rudakov, R. Moyer, S. Krasheninnikov, D. Whyte, G. McKee, G. Tynan, M. Schaffer, P. Stangeby, P. West, S. Allen, T. Evans, R. Fonck, E. Hollmann, A. Leonard, A. Mahdavi, G. Porter, M. Tillack, and G. Antar, Phys. Plasmas **8**, 4826 (2001).
[11]J. A. Boedo, D. L. Rudakov, R. A. Moyer, G. R. McKee, R. J. Colchin, M. J. Schaffer, P. G. Stangeby, W. P. West, S. L. Allen, T. E. Evans, R. J. Fonck, E. M. Hollmann, S. Krasheninnikov, A. W. Leonard, W. Nevins, M. A. Mahdavi, G. D. Porter, G. R. Tynan, D. G. Whyte, and X. Xu, Phys. Plasmas **10**, 1670 (2003).
[12]J. E. Rice, C. Gao, M. L. Reinke, P. H. Diamond, N. T. Howard, H. J. Sun, I. Cziegler, A. E. Hubbard, Y. A. Podpaly, W. L. Rowan, J. L. Terry, M. A. Chilenski, L. Delgado-Aparicio, P. C. Ennever, D. Ernst, M. J. Greenwald, J. W. Hughes, Y. Ma, E. S. Marmar, M. Porkolab, A. E. White, and S. M. Wolfe, Nucl. Fusion **53**, 033004 (2013).
[13]K. Ida, Z. Shi, H. J. Sun, S. Inagaki, K. Kamiya, J. E. Rice, N. Tamura, P. H. Diamond, G. Dif-Pradalier, X. L. Zou, K. Itoh, S. Sugita, T. Estrada, C. Hidalgo, T. S. Hahm, U. Stroth, A. Field, X. T. Ding, Y. Sakamoto, S. Oldenbürger, M. Yoshinuma, T. Kobayashi, M. Jiang, Y. M. Jeon, S. H. Hahn, J. Dong, and S.-I. Itoh, Nucl. Fusion (submitted).
[14]S. Inagaki, T. Tokuzawa, N. Tamura, S. I. Itoh, T. Kobayashi, K. Ida, T. Shimozuma, S. Kubo, K. Tanaka, T. Ido, A. Shimizu, H. Tsuchiya, N. Kasuya, Y. Nagayama, K. Kawahata, S. Sudo, H. Yamada, A. Fujisawa, K. Itoh, and L. E. Group, Nucl. Fusion **53**, 113006 (2013).
[15]T. Kobayashi, K. Itoh, T. Ido, S. I. Itoh, Y. Miura, Y. Nagashima, A. Fujisawa, S. Inagaki, K. Ida, and K. Hoshino, Phys. Rev. Lett. **111**, 035002 (2013).
[16]S. Sugita, K. Itoh, S. I. Itoh, M. Yagi, G. Fuhr, P. Beyer, and S. Benkadda, Plasma Phys. Controlled Fusion **54**, 125001 (2012).
[17]X. Garbet and R. E. Waltz, Phys. Plasmas **5**, 2836 (1998).
[18]T. Hwa and M. Kardar, Phys. Rev. A **45**, 7002 (1992).
[19]P. H. Diamond and T. S. Hahm, Phys. Plasmas **2**, 3640 (1995).
[20]M. E. McIntyre and T. N. Palmer, Nature **305**, 593 (1983).
[21]D. G. Dritschel and M. E. McIntyre, J. Atmos. Sci. **65**, 855 (2008).
[22]G. I. Taylor, Philos. Trans. R. Soc., A **215**, 1 (1915).
[23]P. H. Diamond, Ö. D. Gürcan, T. S. Hahm, K. Miki, Y. Kosuga, and X. Garbet, Plasma Phys. Controlled Fusion **50**, 124018 (2008).
[24]C. McDevitt, P. H. Diamond, O. D. Gürcan, and T. S. Hahm, Phys. Plasmas **17**, 112509 (2010).
[25]Y. Kosuga and P. H. Diamond, Phys. Plasmas **18**, 122305 (2011).
[26]Y. Kosuga and P. H. Diamond, Phys. Plasmas **19**, 072307 (2012).
[27]Y. Kosuga, P. H. Diamond, L. Wang, Ö. D. Gürcan, and T. S. Hahm, Nucl. Fusion **53**, 043008 (2013).
[28]P. B. Rhines, J. Fluid Mech. **69**, 417 (1975).
[29]X. Garbet, Y. Sarazin, F. Imbeaux, P. Ghendrih, C. Bourdelle, O. D. Gürcan, and P. H. Diamond, Phys. Plasmas **14**, 122305 (2007).
[30]Ö. D. Gürcan, P. H. Diamond, X. Garbet, V. Berionni, G. Dif-Pradalier, P. Hennequin, P. Morel, Y. Kosuga, and L. Vermare, Phys. plasmas **20**, 022307 (2013).
[31]Y. Kosuga, P. H. Diamond, and Ö. D. Gürcan, Phys. Rev. Lett. **110**, 105002 (2013).
[32]G. B. Whitham, *Linear and Nonlinear Waves* (Wiley-Interscience, New York, 1999).
[33]M. R. Flynn, A. R. Kasimov, J. C. Nave, R. R. Rosales, and B. Seibold, Phys. Rev. E **79**, 056113 (2009).
[34]B. A. Carreras, D. Newman, V. E. Lynch, and P. H. Diamond, Phys. Plasmas **3**, 4106 (1996).
[35]D. Helbing, Phys. Rev. E **59**, R2505 (1999).
[36]P. H. Diamond, S.-I. Itoh, and K. Itoh, *Modern Plasma Physics Volume1: Physical Kinetics of Turbulent Plasmas* (Cambridge University Press, Cambridge, 2011).
[37]B. B. Kadomtsev and O. P. Pogutse, *Reviews of Plasma Physics*, edited by M. A. Leontovich (Consultants Bureau, 1970), Vol. 5.
[38]H. Biglari, P. H. Diamond, and P. W. Terry, Phys. Fluids **31**, 2644 (1988).
[39]Z. Guo, P. H. Diamond, Y. Kosuga, and O. D. Gürcan, Phys. Rev. E **89**, 041101(R) (2014).
[40]L. P. Pitaevskii and E. M. Lifshitz, *Physical Kinetics: Course of Theoretical Physics* (Pergamon, Oxford, 1981).
[41]K. H. Burrell, Phys. Plasmas **4**, 1499 (1997).
[42]G. Dif-Pradalier, 7th Festival de Theorie, Aix-en-Provence, France, 2013.
[43]P. H. Diamond, V. B. Lebedev, D. E. Newman, and B. A. Carreras, Phys. Plasmas **2**, 3685 (1995).
[44]T. S. Hahm, P. H. Diamond, Z. Lin, S.-I. Itoh, and K. Itoh, Plasma Phys. Controlled Fusion **46**, A323 (2004).
[45]T. S. Hahm, P. H. Diamond, Z. Lin, G. Rewoldt, Ö. D. Gürcan, and S. Ethier, Phys. Plasmas **12**, 090903 (2005).
[46]Ö. D. Gürcan, P. H. Diamond, T. S. Hahm, and Z. Lin, Phys. Plasmas **12**, 032303 (2005).